Supporting Information

Chang et al. 10.1073/pnas.1117837109

SI Materials and Methods

Electron Microscopy. Electron microscopy was performed as previously described (1, 2).

Spermatozoa Staining and FACS. Acridine orange (AO) and propidium iodide staining of caudal spermatozoa and subsequent analyses by FACS were performed as previously described (3).

Acid-Urea Polyacrylamide Gel Electrophoresis. Isolation of basic nuclear proteins and acid-urea polyacrylamide gel electrophoresis were performed as described (3) with modifications. Briefly, testis lysates or sonication-resistant spermatids prepared by sonication were extracted with 0.25% HCl (vol/vol) and precipitated with 3.5% trichloroacetic acid (TCA; wt/vol) overnight. Supernatants were precipitated with 25% TCA (wt/vol), and the resulting precipitates were washed with acidified acetone and then acetone, and dried. Samples were resolved on a 15% acid-urea polyacrylamide gel, and bands were visualized by Coomassie blue staining.

Polysome and mRNA Localization Analyses. Postnuclear total testis lysates were prepared by Dounce homogenization in polysome extraction buffer (PEB) [60 mM NaCl, 15 mM Tris·HCl, pH 7.5, 15 mM $MgCl_2$, 0.5% Triton X-100, 100 μg/mL cycloheximide (CHX), 1 mg/mL heparin]. Cell lysates were prepared by addition of PEB and scraping. Lysates were layered over a 10–50% sucrose gradient (wt/vol) and centrifuged at 36,000 rpm on the SW 41 rotor (Beckman Coulter) for 2 h 15 min at 4 °C. Fractions were collected from the top of the gradient and A_{254} for each fraction was measured. RNA was extracted from 10% of total lysates and 20% of each fraction and analyzed by quantitative (Q)RT-PCR. Expression levels are represented as the percentage of transcript in each fraction compared with total lysate.

Microarray. Total testis RNA was hybridized to an Agilent 4 × 44k Whole Mouse Genome Microarray according to the manufacturer's protocol and scanned on an Agilent G2505B scanner. Expression levels of selected genes were further verified by QRT-PCR analyses on RNA extracted from purified round spermatids.

Ribonucleoprotein Capture Assay. Ribonucleoprotein (RNP) capture assay was performed as previously described (4). Briefly, 2% of four RNP or five polysome fractions isolated by sucrose gradient was pooled and incubated with 100 μL blocked oligo(dT)-cellulose [10 mg oligo(dT)-cellulose] beads blocked for 1 h at 4 °C by incubating with binding buffer [50 mM Hepes, pH 7.5, 150 mM KOAc, 5 mM $Mg(OAc)_2$, 2 mM DTT with 5% BSA] for 30 min at 4 °C with agitation. Beads were collected by centrifugation at 500 × *g* and washed twice with binding buffer, and bound proteins were eluted by boiling in Laemmli sample buffer. Twenty percent of input and bound proteins was analyzed by Western blot.

Plasmids. *Prm1* 3′ UTR template for in vitro transcribed ^{32}P-labeled riboprobe was generated by cloning the amplified *Prm1* 3′ UTR into SpeI-SacI sites in pBluescript (Stratagene). Luciferase 3′ UTR constructs were generated by PCR amplification of genomic DNA isolated from mouse tissue using primers described in Table S3 and cloning into SpeI-SacI sites of pMIR-REPORT luciferase (Applied Biosystems). pcDNA3.1 (vector; Invitrogen), pCMV6-Entry|*Arpc5*-Myc-DDK (FLAG-Arpc5; Origene), and pRL-CMV (Renilla luciferase; Promega) are commercially available.

RNA-Electrophoretic Mobility Shift Assay. ^{32}P-radiolabeled mouse *Prm1* 3′ UTR riboprobe (using SacI-digested linearized pBluescript|*Prm1* 3′ UTR construct as template) was prepared by in vitro transcription as described previously (5). For gel shift assay, 10 μg recombinant Arpc5 or 10 μg BSA was incubated with 100,000 counts of ^{32}P-labeled probe for 20 min on ice in electrophoretic mobility shift assay (EMSA) buffer (20 mM Hepes, pH 7.6, 75 mM NaCl, 1.5 mM KCl, 5 mM $MgCl_2$, 175 mM sucrose, 2 mM DTT). For supershift assay, 10 μg postnuclear total testis lysate was preincubated with 5 μg of the appropriate antibody for 30 min on ice in EMSA buffer. Then, 100,000 counts of ^{32}P-labeled probe was added and incubated for an additional 20 min on ice. Unincorporated probe was digested with RNase A and T_1 for 20 min at 30 °C. Samples were UV–cross-linked and resolved on a 6% native acrylamide gel.

[^{35}S]Methionine Incorporation. HeLa cells were transfected with 500 ng pcDNA3.1 or pCMV6-Entry|*Arpc5*-Myc-DDK. After 48 h, cells were washed twice with 1× PBS and incubated with methionine/cysteine-free media for 3 h at 37 °C. Cells were trypsinized, counted, and resuspended in methionine/cysteine-free media. [^{35}S]Methionine was added to 200,000 cells. After the indicated times, cells were washed twice with 1× PBS and protein was extracted using 10% TCA (wt/vol), boiled, and placed on ice. Protein precipitates were collected on GF/C filters (Whatman), washed twice with 5% TCA (wt/vol), once with 70% ethanol (vol/vol), and once with cold acetone. Filters were placed in scintillation fluid and cpm was quantified.

In Vitro Translation Assay. In vitro translation assays were performed as described previously (6). Briefly, the indicated amounts of purified recombinant Arpc5 or BSA in MES buffer (20 mM MES, pH 6.0, 200 mM NaCl, 2 mM DTT, 10% glycerol) were added to the Rabbit Reticulocyte Lysate System (Promega). Extracts were programmed with 100 ng capped luciferase mRNA, in vitro transcribed using the mScript mRNA Production System (Epicentre). Reactions were incubated for 30 min at 30 °C, and luciferase activities were quantitated using the Dual-Luciferase Reporter Assay System (Promega). To examine 80S and 48S formation, reactions were preincubated with 10 μg recombinant Arpc5 or BSA for 10 min on ice, followed by incubation with 1 mM CHX or 0.5 mM GMP-PNP for 3 min at 30 °C. Extracts were then programmed with 20,000 counts of ^{32}P-radiolabeled and capped mRNA and incubated for 20 min at 30 °C. Translation was monitored by fractionation using a 10–30% sucrose gradient (wt/vol), followed by scintillation counting.

Coimmunofluorescence and RNA Colocalization. For the localization of endogenous proteins, Arpc5 in NIH 3T3 cells was visualized using anti-Arpc5 (1:100; Abcam) followed by Alexa Fluor 488-conjugated goat anti-rabbit (green). Endogenous GW182 was visualized using anti-GW182 (1:100; Santa Cruz Biotechnology) followed by Cy3-conjugated goat anti-mouse (red). DAPI was used to stain nuclei (blue). To examine the effect of Arpc5 overexpression, HeLa cells were cotransfected with 500 ng vector or FLAG-Arpc5. After 24 h, cells were trypsinized and counted, and 50,000 were placed on coated microscope slides. Forty-eight hours after transfection, slides were fixed in 4% paraformaldehyde, blocked with 10% goat serum, and incubated with human GW182 antiserum 18033 followed by Alexa Fluor 488-conjugated goat anti-human antibody (Invitrogen). Slides were then incubated with anti-FLAG (Sigma) followed by Cy3-conjugated goat anti-mouse antibody (Zymed). RNA colocalization studies were performed as described (7).

1. Rao MK, et al. (2006) Tissue-specific RNAi reveals that WT1 expression in nurse cells controls germ cell survival and spermatogenesis. *Genes Dev* 20(2):147–152.
2. Sinha-Hikim AP, Swerdloff RS (1993) Temporal and stage-specific changes in spermatogenesis of rat after gonadotropin deprivation by a potent gonadotropin-releasing hormone antagonist treatment. *Endocrinology* 133:2161–2170.
3. Zhao M, et al. (2001) Targeted disruption of the transition protein 2 gene affects sperm chromatin structure and reduces fertility in mice. *Mol Cell Biol* 21:7243–7255.
4. Grivna ST, Pyhtila B, Lin H (2006) MIWI associates with translational machinery and PIWI-interacting RNAs (piRNAs) in regulating spermatogenesis. *Proc Natl Acad Sci USA* 103:13415–13420.
5. Chang YF, Chan WK, Imam JS, Wilkinson MF (2007) Alternatively spliced T-cell receptor transcripts are up-regulated in response to disruption of either splicing elements or reading frame. *J Biol Chem* 282:29738–29747.
6. Coller J, Parker R (2005) General translational repression by activators of mRNA decapping. *Cell* 122:875–886.
7. Lee EK, et al. (2010) hnRNP C promotes APP translation by competing with FMRP for APP mRNA recruitment to P bodies. *Nat Struct Mol Biol* 17:732–739.

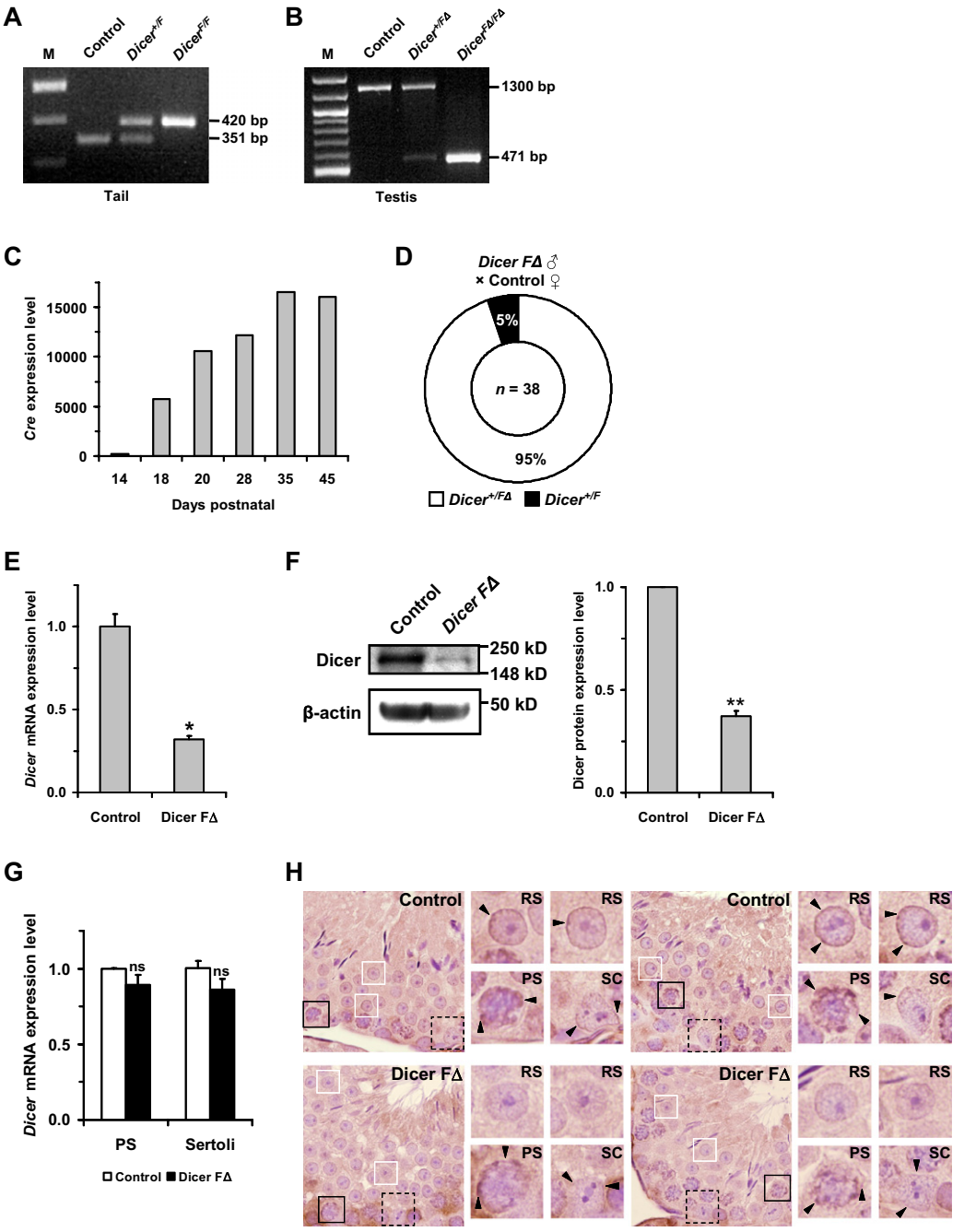

Fig. S1. Efficiency of *Prm1-cre*–mediated recombination and Dicer knockdown in postmeiotic germ cells. (*A* and *B*) PCR genotype analyses of tail genomic DNA using primers F1 and R1, and testis genomic DNA using primers F1 and R2 as in Fig. 1*A*. Sequences and product sizes have been previously described (1). M, molecular weight marker. (*C*) QRT-PCR analyses of *cre* expression in the testes of *Prm1-cre* mice. *Prm1-cre* transgene expression began on postnatal day 18, in accordance with when round spermatids are first observed in mouse seminiferous epithelium (2). (*D*) Chart showing pup genotype percentages from matings between *Dicer FΔ* male and control female mice. (*E*) QRT-PCR analyses of RNA isolated from purified round spermatids show significantly reduced (albeit not completely absent) levels of Dicer in *Dicer FΔ* testes ($n = 3$; $^*P < 0.05$). (*F*) Western blot analyses using anti-Dicer (1:200; Santa Cruz Biotechnology) antibody further confirmed QRT-PCR results shown in *E*. Anti–β-actin (1:5,000; Sigma) was used as a loading control. Gel photographs are representative of three independent experiments (*Left*). Band intensities were quantified using ImageJ software (http://imagej.nih.gov/ij) and plotted (*Right*) (3) ($n = 3$; $^{**}P < 0.005$). (*G*) QRT-PCR analyses of RNA isolated from purified pachytene spermatocytes (PS) or Sertoli cells show no change in Dicer levels between control and *Dicer FΔ* testes [$n = 3$; no significant change (ns)]. For *E*–*G*, isolation of germ/Sertoli cell populations was performed using a centrifugal elutriation approach, and purity was determined by microscopic examination combined with QRT-PCR analyses using cell type-specific markers as previously described (4). Only germ/Sertoli cell preparations with ≥90% purity were used for subsequent RNA and protein analyses ($n = 3$; pooled from four control or *Dicer FΔ* mice for each replicate). Please note that ∼25% of Dicer (∼10% contamination from other cell types subtracted from ∼35% as quantified by QRT-PCR and Western blot analyses) is still present in *Dicer FΔ* round spermatids. (*H*) Immunohistochemical analyses (anti-Dicer, 1:100; Abcam) showing cytoplasmic (perinuclear) expression of Dicer (arrowheads) in testis sections. In agreement with QRT-PCR (*E*) and Western blot (*F*) results, the vast majority of round spermatids (RS) in *Dicer FΔ* testis sections lacked the Dicer staining observed in control testis sections (white boxes, magnified views *Right*), although some round spermatids in *Dicer FΔ* testis sections displayed minimal Dicer staining, suggesting that residual Dicer protein was present in these cells. Consistent with QRT-PCR results shown above (*G*), Dicer staining in spermatocytes (PS; black solid boxes, magnified views *Right*) and Sertoli cells (SC; black dashed boxes, magnified views *Right*) were similar in control and *Dicer FΔ* testis sections.

1. Harfe BD, McManus MT, Mansfield JH, Hornstein E, Tabin CJ (2005) The RNaseIII enzyme Dicer is required for morphogenesis but not patterning of the vertebrate limb. *Proc Natl Acad Sci USA* 102:10898–10903.
2. Bellvé AR, et al. (1977) Spermatogenic cells of the prepuberal mouse. Isolation and morphological characterization. *J Cell Biol* 74(1):68–85.
3. Abramoff MD, Magalhaes PJ, Ram SJ (2004) Image processing with ImageJ. *Biophotonics Int* 11(7):36–42.
4. Chang YF, Lee-Chang JS, Panneerdoss S, MacLean JA, II, Rao MK (2011) Isolation of Sertoli, Leydig, and spermatogenic cells from the mouse testis. *Biotechniques* 51:341–344.

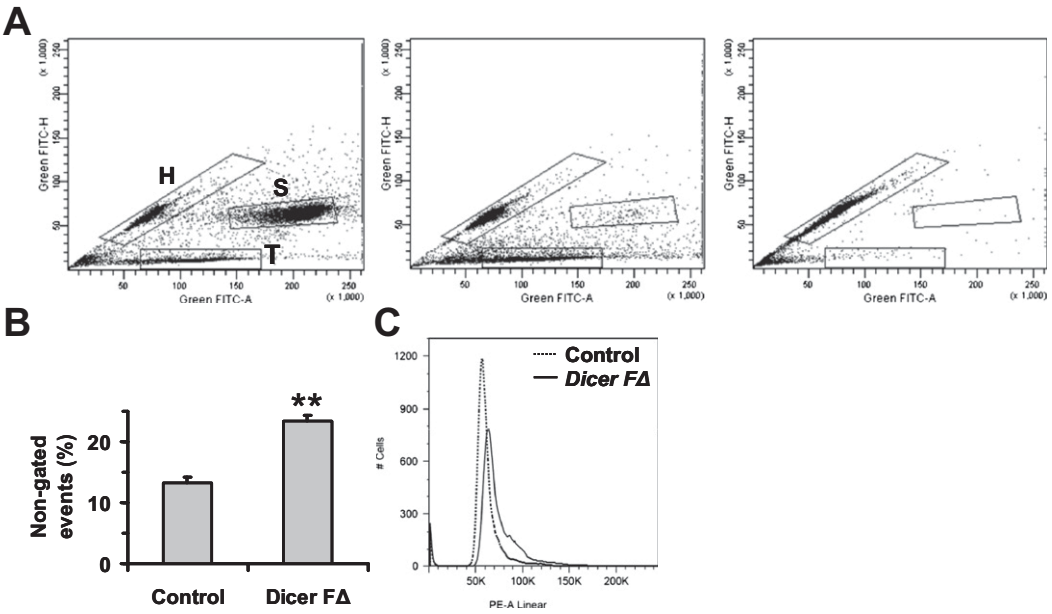

Fig. S2. FACS analyses of AO- and PI-stained sperm heads. (*A*) Sperm from control mice were untreated (*Left*), treated with trypsin (*Center*), or sonicated (*Right*) and subjected to AO staining (1) followed by FACS. Regions containing intact sperm (S), free sperm heads (H), and free sperm tails (T) are marked. Gated sperm heads are further analyzed in Fig. 2 *B* and *C*. (*B*) Percentage of nongated/total events in Fig. 2*C* ($n = 3$; $^{**}P < 0.005$). (*C*) FACS of sonicated PI-stained sperm heads. PI intercalates partially compacted DNA more efficiently (2).

1. Zhao M, et al. (2001) Targeted disruption of the transition protein 2 gene affects sperm chromatin structure and reduces fertility in mice. *Mol Cell Biol* 21:7243–7255.
2. Mátyus L, Szabó G, Jr., Resli I, Gáspár R, Jr., Damjanovich S (1984) Flow cytometric analysis of viability of bull sperm cells. *Acta Biochim Biophys Acad Sci Hung* 19:209–214.

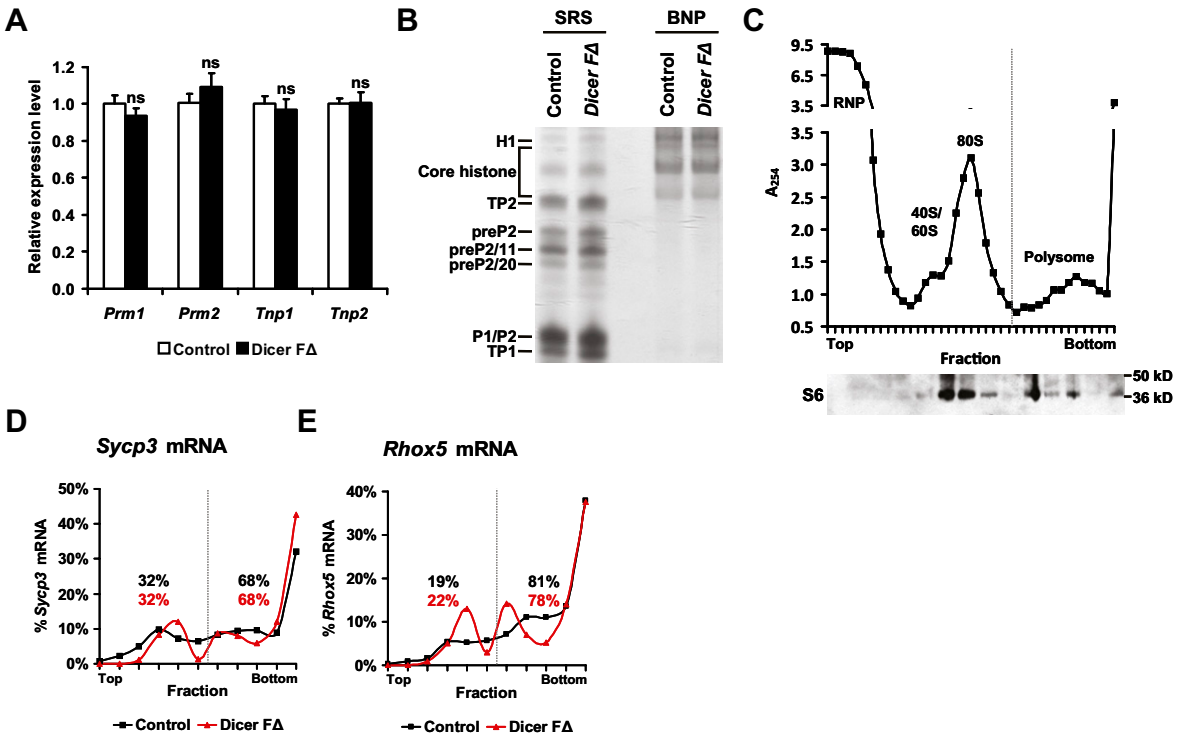

Fig. S3. Steady-state mRNA levels and testis basic nuclear protein (BNP) processing are not altered in *Dicer FΔ* mice. (*A*) QRT-PCR analyses of total testis RNA using primers described in Table S3. Expression levels are normalized to Rpl19 ($n = 5$). (*B*) Acid-urea polyacrylamide gel electrophoresis of TCA-extracted basic nuclear proteins from total testis (BNP) and sonication-resistant spermatids (SRS). H1, histone H1; P1, protamine 1; P2, protamine 2; TP1, transition protein 1; TP2, transition protein 2. (*C*) Polysome profile of postnuclear total testis lysate, fractionated, and A_{254} measured (*Upper*). Western blots on pooled fractions were performed using anti-S6 (*Lower*). Dotted line indicates separation between complexes. (*D* and *E*) QRT-PCR of fractionated lysates was performed using the indicated primers. Dotted line indicates separation between complexes. Percentages indicate the amount of the specified mRNA in the fraction compared with the total amount of the specified mRNA in all fractions.

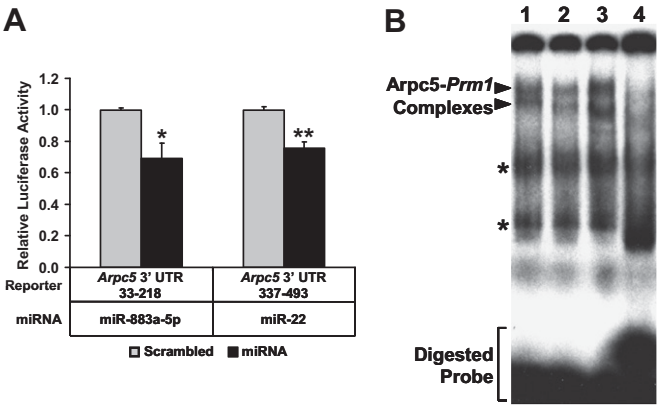

Fig. S4. Arpc5 is targeted by miR-22/883a-5p and interacts with *Prm1* mRNA. (*A*) Validation of Arpc5 as a miR-22/883a-5p target. HeLa cells cotransfected with indicated luciferase-Arpc5 3′ UTR construct and miRNA mimic (100 nM; Qiagen). Values are normalized against Renilla luciferase activity ($n = 4$; $^*P < 0.05$, $^{**}P < 0.005$). (*B*) RNA-EMSA supershift of postnuclear total testis lysate using in vitro transcribed radiolabeled *Prm1* 3′ UTR riboprobe and anti-Arpc5 antibody. For supershift/retardation of observed complexes, control IgG (mouse, lane 1; rabbit, lane 2; Santa Cruz Biotechnology), anti-TRBP (lane 3), or anti-Arpc5 (lane 4) antibodies were incubated with lysate before addition of radiolabeled probe. Arrowheads indicate relevant complexes inhibited by anti-Arpc5 preincubation. Stars indicate nonspecific complexes. Supershift assay with commercially available antibody against TRBP, which is known to interact with *Prm1* 3′ UTR (1), did not result in clear migration/inhibition of any relevant protein–RNA complexes. Although one band just below complex II in the anti-TRBP lane (lane 3) was always observed, it was not clear from which complex this band originated. Gel photograph is representative of three independent experiments.

1. Lee K, Fajardo MA, Braun RE (1996) A testis cytoplasmic RNA-binding protein that has the properties of a translational repressor. *Mol Cell Biol* 16:3023–3034.

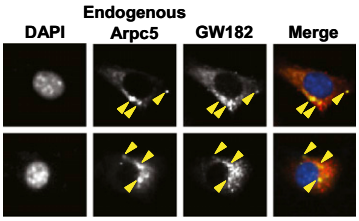

Fig. S5. Endogenous Arpc5 colocalizes with P-body marker GW182. Endogenous Arpc5 (green), endogenous GW182 (red), and nuclei (blue), shown in black and white for clarity. Arrowheads indicate merge of green and red signals (yellow).

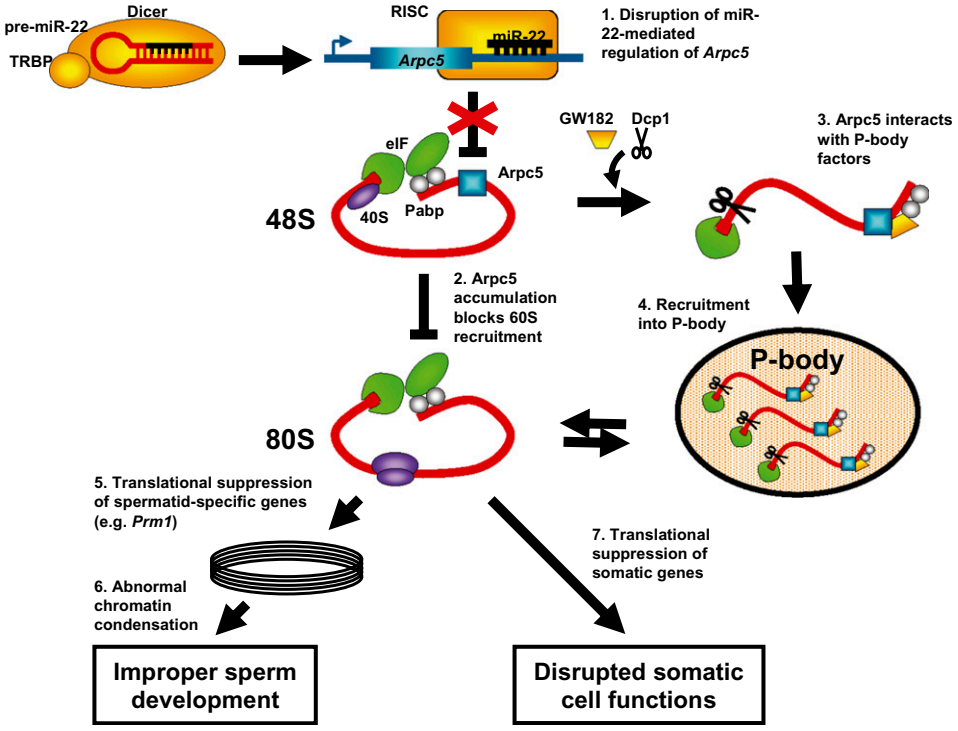

Fig. S6. Model of microRNA (miRNA)/Arpc5 action in the posttranscriptional gene regulation of germ/somatic cells. Finely controlled temporal gene expression is essential for proper spermatid differentiation as well as diverse cellular functions in somatic cells (1–3). We posit that miRNA-mediated (e.g., miR-22/883a-5p) translational regulation plays an important role in this process, as it controls the expression of checkpoint regulator genes such as Arpc5 (4), which regulates the distribution of localizing mRNAs into translationally active polysomes and translationally inert RNP complexes. Our results suggest that loss of miRNA-dependent regulation leading to Arpc5 overexpression interferes with translation initiation by preventing joining of 60S to the 48S preinitiation complex (5). We posit that association of Arpc5 to germ/somatic cell mRNA 3′ UTRs may result in the recruitment of corepressors that interact with the preinitiation complex and compete with the binding of translation initiation machinery. It is also likely that Arpc5–mRNP complex association with chromatoid/P-body proteins (6) may facilitate bound mRNAs to directly contact the translational suppression machinery (7). RISC, RNA-Induced Silencing Complex; eIF, eukaryotic translation initiation factor.

1. Chang YF, Chan WK, Imam JS, Wilkinson MF (2007) Alternatively spliced T-cell receptor transcripts are up-regulated in response to disruption of either splicing elements or reading frame. *J Biol Chem* 282:29738–29747.
2. Coller J, Parker R (2005) General translational repression by activators of mRNA decapping. *Cell* 122:875–886.
3. Lee EK, et al. (2010) hnRNP C promotes APP translation by competing with FMRP for APP mRNA recruitment to P bodies. *Nat Struct Mol Biol* 17:732–739.
4. Rao MK, et al. (2006) Tissue-specific RNAi reveals that WT1 expression in nurse cells controls germ cell survival and spermatogenesis. *Genes Dev* 20:147–152.
5. Sinha-Hikim AP, Swerdloff RS (1993) Temporal and stage-specific changes in spermatogenesis of rat after gonadotropin deprivation by a potent gonadotropin-releasing hormone antagonist treatment. *Endocrinology* 133:2161–2170.
6. Zhao M, et al. (2001) Targeted disruption of the transition protein 2 gene affects sperm chromatin structure and reduces fertility in mice. *Mol Cell Biol* 21:7243–7255.
7. Grivna ST, Pyhtila B, Lin H (2006) MIWI associates with translational machinery and PIWI-interacting RNAs (piRNAs) in regulating spermatogenesis. *Proc Natl Acad Sci USA* 103: 13415–13420.

Table S1. Epididymal sperm morphology

Morphology	Control (%)	Dicer FΔ(%)
Normal	91.2 ± 1.2	82.0 ± 2.1*
Abnormal	10.1 ± 1.2	18.0 ± 2.1*
Rounded or bent head	5.2 ± 0.6	10.8 ± 1.5*
Two-headed	0.1 ± 0.1	1.0 ± 0.2*
Kinked or other tail abnormalities	4.8 ± 0.8	6.3 ± 1.3

Caudal epididymal sperm from three control and three *Dicer FΔ* mice were counted in triplicate. At least 1,000 total spermatozoa were counted for each mouse.
*$P < 0.05$.

Table S2. Highly altered genes in *Dicer FΔ* postmeiotic germ cells

Gene	Fold change	Function and expression	Refs.
Arpc5	7.59	Involved in vesicle trafficking and cell polarity by stimulating actin filament assembly	(1–3)
Catsperb	2.05	Required for sperm hyperactivation; testis-restricted expression in spermatocytes and spermatids	(4)
Ddr2	−3.56*	May function in endocrine regulation of the testis; deletion causes sterility	(5)
Fus	−2.53*	Assists in chromosome pairing during meiosis and may also play a role in DNA repair; knockout males are sterile	(6, 7)
Grtp1	2.60	Possible function in cell cycle and mitosis; expression is most abundant in testis and increases postpuberty	(8)
Gsr	3.34	Protects sperm from reactive oxygen species through glutathione recycling	(9, 10)
Gss	2.75	Protects sperm from reactive oxygen species through glutathione synthesis	(9, 10)
Map2k7	36.48	Activator of the JNK pathway and downstream target of Rac1; testis-restricted expression of an alternatively spliced transcript	(11, 12)
Ptpro	−2.41*	Receptor-type tyrosine protein phosphatase negatively regulated by estrogen and down-regulated by the miR-17-92 cluster; highly expressed in testis	(13, 14)
Ptprv	37.87	Receptor-type tyrosine protein phosphatase with a possible role in the dissociation of the blood–testis barrier; expressed in Sertoli cells	(15, 16)
Sord	2.01	Allows sorbitol to be used as an energy source for sperm motility and capacitation; may be posttranscriptionally regulated	(17)
Spata7	−2.40*	Unknown function; testis-restricted expression in primary spermatocytes	(18)
Stk25	−2.22*	Involved in perinuclear localization of Golgi and may control cell polarity; highly expressed in testis	(19, 20)

Genes listed were found to be highly altered (up-regulated or down-regulated) in *Dicer FΔ* mice testis. Values in "fold change" column represent validation of microarray data (independent analyses of total testis RNA of two control and two *Dicer FΔ* mice) using QRT-PCR unless stated. QRT-PCR analyses were performed on purified round spermatid RNA pooled from four mice.
*Value from microarray analyses.

1. Fucini RV, Chen JL, Sharma C, Kessels MM, Stamnes M (2002) Golgi vesicle proteins are linked to the assembly of an actin complex defined by mAbp1. *Mol Biol Cell* 13:621–631.
2. Goley ED, Welch MD (2006) The ARP2/3 complex: An actin nucleator comes of age. *Nat Rev Mol Cell Biol* 7:713–726.
3. Luna A, et al. (2002) Regulation of protein transport from the Golgi complex to the endoplasmic reticulum by CDC42 and N-WASP. *Mol Biol Cell* 13:866–879.
4. Liu J, Xia J, Cho KH, Clapham DE, Ren D (2007) CatSperβ, a novel transmembrane protein in the CatSper channel complex. *J Biol Chem* 282:18945–18952.
5. Kano K, et al. (2008) A novel dwarfism with gonadal dysfunction due to loss-of-function allele of the collagen receptor gene, Ddr2, in the mouse. *Mol Endocrinol* 22:1866–1880.
6. Kuroda M, et al. (2000) Male sterility and enhanced radiation sensitivity in TLS(−/−) mice. *EMBO J* 19:453–462.
7. Lerga A, et al. (2001) Identification of an RNA binding specificity for the potential splicing factor TLS. *J Biol Chem* 276:6807–6816.
8. Lu C, et al. (2001) Grtp1, a novel gene regulated by growth hormone. *Endocrinology* 142:4568–4571.
9. Luberda Z (2005) The role of glutathione in mammalian gametes. *Reprod Biol* 5(1):5–17.
10. Meister A (1988) Glutathione metabolism and its selective modification. *J Biol Chem* 263:17205–17208.
11. Holland PM, Suzanne M, Campbell JS, Noselli S, Cooper JA (1997) MKK7 is a stress-activated mitogen-activated protein kinase kinase functionally related to hemipterous. *J Biol Chem* 272:24994–24998.
12. Tournier C, Whitmarsh AJ, Cavanagh J, Barrett T, Davis RJ (1997) Mitogen-activated protein kinase kinase 7 is an activator of the c-Jun NH_2-terminal kinase. *Proc Natl Acad Sci USA* 94:7337–7342.
13. Ramaswamy B, et al. (2009) Estrogen-mediated suppression of the gene encoding protein tyrosine phosphatase PTPRO in human breast cancer: Mechanism and role in tamoxifen sensitivity. *Mol Endocrinol* 23(2):176–187.
14. Xu X, et al. (2008) Protein tyrosine phosphatase receptor-type O (PTPRO) is co-regulated by E2F1 and miR-17-92. *FEBS Lett* 582:2850–2856.
15. Dacquin R, et al. (2004) Knock-in of nuclear localised β-galactosidase reveals that the tyrosine phosphatase Ptprv is specifically expressed in cells of the bone collar. *Dev Dyn* 229:826–834.
16. Mauro LJ, et al. (1994) Identification of a hormonally regulated protein tyrosine phosphatase associated with bone and testicular differentiation. *J Biol Chem* 269:30659–30667.
17. Cao W, Aghajanian HK, Haig-Ladewig LA, Gerton GL (2009) Sorbitol can fuel mouse sperm motility and protein tyrosine phosphorylation via sorbitol dehydrogenase. *Biol Reprod* 80(1):124–133.
18. Zhang X, et al. (2003) A novel gene, RSD-3/HSD-3.1, encodes a meiotic-related protein expressed in rat and human testis. *J Mol Med (Berl)* 81:380–387.
19. Osada S, et al. (1997) YSK1, a novel mammalian protein kinase structurally related to Ste20 and SPS1, but is not involved in the known MAPK pathways. *Oncogene* 14:2047–2057.
20. Preisinger C, et al. (2004) YSK1 is activated by the Golgi matrix protein GM130 and plays a role in cell migration through its substrate 14-3-3ζ. *J Cell Biol* 164:1009–1020.

Table S3. Primers used in this study

Primer	Species	Type	Sequence
Acrv1	Mouse	QRT-PCR	5′-TCAGCAACTTTCAAGCGAGTAT-3′
			5′-CTCCTGAAGAGTGCTCACCTG-3′
Arpc5	Mouse	QRT-PCR	5′-GTGCAGGCAGCATCGTCTT-3′
			5′-CATTAGGAGGTCCACACCGTT-3′
Catsperb	Mouse	QRT-PCR	5′-AGGTTCATCGTTTCAAGTTTCCAGTCAC-3′
			5′-ACAGTTGTACTTGAGGTGAGTCCAG-3′
cre	P1 bacteriophage	QRT-PCR	5′-GCGGTCTGGCAGTAAAAACTATC-3′
			5′-GTGAAACAGCATTGCTGTCACTT-3′
Dbil5	Mouse	QRT-PCR	5′-CCCAGGGCGACTGTAACATC-3′
			5′-GCAATGTAGATCCTCATGGCAT-3′
Grtp1	Mouse	QRT-PCR	5′-TCGATCCGTATGGGTTTGAAAG-3′
			5′-TCGCCCTCTTGGTGAGTATCA-3′
Dicer1	Mouse	QRT-PCR	5′-GGTCCTTTCTTTGGACTGCCA-3′
			5′-GCGATGAACGTCTTCCCTGA-3′
Gsr	Mouse	QRT-PCR	5′-CCACGGCTATGCAACATTCG-3′
			5′-GATCTGGCTCTCGTGAGGAA-3′
Gss	Mouse	QRT-PCR	5′-CAAAGCAGGCCATAGACAGGG-3′
			5′-AAAAGCGTGAATGGGGCATAC-3′
Hp	Mouse	QRT-PCR	5′-GCTATGTGGAGCACTTGGTTC-3′
			5′-CACCCATTGCTTCTCGTCGTT-3′
Map2k7	Mouse	QRT-PCR	5′-ATGGAGAGCATCGAGATTGACC-3′
			5′-CGCCGCATTTGCTTAACAG-3′
Prm1	Mouse	QRT-PCR	5′-CCGTCGCAGGCGAAGATGTC-3′
			5′-CACCTTATGGTGTATGAGCGG-3′
Prm2	Mouse	QRT-PCR	5′-GCTGCTCTCGTAAGAGGCTACA-3′
			5′-AGTGATGGTGCCTCCTACATTT-3′
Ptprv	Mouse	QRT-PCR	5′-CCAGGACTCTTTGGCCCAG-3′
			5′-AGGGCATAGTCAAATCCACCT-3′
Rhox5	Mouse	QRT-PCR	5′-CACCAGGACCAAAGTGGCC-3′
			5′-GGTATGGAAGCTGAGGGTT-3′
Rpl19	Mouse	QRT-PCR	5′-CTGAAGGTCAAAGGGAATGTG-3′
			5′-GGACAGAGTCTTGATGATCTC-3′
Sord	Mouse	QRT-PCR	5′-TGGGAGCATGGACGAATTGG-3′
			5′-CAACCCGATCTCCTGGTTTCA-3′
Sult1e1	Mouse	QRT-PCR	5′-ATGGAGACTTCTATGCCTGAGT-3′
			5′-ACACAACTTCACTAATCCAGGTG-3′
Sycp3	Mouse	QRT-PCR	5′-AGCCAGTAACCAGAAAATTGAGC-3′
			5′-CCACTGCTGCAACACATTCATA-3′
Tnp1	Mouse	QRT-PCR	5′-GAGAGGTGGAAGCAAGAGAAAA-3′
			5′-CCCACTCTGATAGGATCTTTGG-3′
Tnp2	Mouse	QRT-PCR	5′-GAAGGGAAAGTGAGCAAGAGAA-3′
			5′-GCATAGAAATTGCTGCAGTGAC-3′
let-7i*	Mouse	QRT-PCR	5′-CTGCGCAAGCTACTGC-3′
miR-22	Mouse	QRT-PCR	5′-AAGCTGCCAGTTGAAGAA-3′
miR-24	Mouse	QRT-PCR	5′-CTCAGTTCAGCAGGAACA-3′
miR-34a	Mouse	QRT-PCR	5′-TGGCAGTGTCTTAGC-3′
miR-127	Mouse	QRT-PCR	5′-TCGGATCCGTCTGAGCT-3′
miR-143	Mouse	QRT-PCR	5′-TGAGATGAAGCACTGTAGCTC-3′
miR-201	Mouse	QRT-PCR	5′-TACTCAGTAAGGCATTGTTCTT-3′
miR-741	Mouse	QRT-PCR	5′-TGAGAGATGCCATTCTATGTA-3′
miR-744	Mouse	QRT-PCR	5′-GGGCTAGGGCTAACAGCA-3′
miR-883a-5p	Mouse	QRT-PCR	5′-TGCTGAGAGAAGTAGCAGTT-3′
Snora74a (U19)	Mouse	QRT-PCR	5′-TGTGGTGCCCGAGATCGT-3′
			5′-TGGGAGCCGACCCTTAGTAA-3′
Arpc5 3′ UTR 33–218	Mouse	Cloning	5′-GGACTAGTGGGAGTTGCTGGTATAAAGACC-3′
			5′-CGAGCTCCAAACATCCCCACTGAGAC-3′
Arpc5 3′ UTR 337–493	Mouse	Cloning	5′-GGACTAGTCTGAGAGATGTGATCAAAGTTG-3′
			5′-CGAGCTCCTACTTGCCCTGGAAACAC-3′
Prm1 3′ UTR 69–152	Mouse	Cloning	5′-GGACTAGTCACATCTTGAAAAATGCCAC-3′
			5′-CGAGCTCGAGTTTTCAACATTTATTGACAG-3′

Primer sequences were obtained from PrimerBank (1).

1. Spandidos A, Wang X, Wang H, Seed B (2010) PrimerBank: A resource of human and mouse PCR primer pairs for gene expression detection and quantification. *Nucleic Acids Res* 38(Database issue):D792–D799.